

Estimating Human Movement Parameters Using a Software Radio-based Radar

Bruhtesfa Godana*, André Barroso†, Geert Leus‡

* Norwegian University of Science and Technology, Trondheim, Norway

†Philips Research Europe, Eindhoven, The Netherlands

‡Faculty of EEMCS, Delft University of Technology, Delft, The Netherlands

*godana@iet.ntnu.no, †andre.barroso@philips.com, ‡g.j.t.leus@tudelft.nl

Abstract—Radar is an attractive technology for long term monitoring of human movement as it operates remotely, can be placed behind walls and is able to monitor a large area depending on its operating parameters. A radar signal reflected off a moving person carries rich information on his or her activity pattern in the form of a set of Doppler frequency signatures produced by the specific combination of limbs and torso movements. To enable classification and efficient storage and transmission of movement data, unique parameters have to be extracted from the Doppler signatures. Two of the most important human movement parameters for activity identification and classification are the velocity profile and the fundamental cadence frequency of the movement pattern. However, the complicated pattern of limbs and torso movement worsened by multipath propagation in indoor environment poses a challenge for the extraction of these human movement parameters. In this paper, three new approaches for the estimation of human walking velocity profile in indoor environment are proposed and discussed. The first two methods are based on spectrogram estimates whereas the third method is based on phase difference computation. In addition, a method to estimate the fundamental cadence frequency of the gait is suggested and discussed. The accuracy of the methods are evaluated and compared in an indoor experiment using a flexible and low-cost software defined radar platform. The results obtained indicate that the velocity estimation methods are able to estimate the velocity profile of the person's translational motion with an error of less than 10%. The results also showed that the fundamental cadence is estimated with an error of 7%.

Index Terms—Human motion, Human gait, Velocity profile, Cadence frequency, Radar, GNU Radio

I. INTRODUCTION

Automatic classification of human activity is an enabler of relevant applications in the healthcare and wellness domains given the strong empirical relation between a person's health and his or her activity profile. As a rule of thumb, the ability of a person to engage independently in strenuous and complex activities entails better fitness and health status, the reverse relation being also generally true. This implication has inspired the design of activity monitoring systems that range from fitness training [3] to early discharge support of postoperative patients [4]. Seniors living independently by wish or circumstances may also benefit from remote activity classification as a means of assessing their health status or identifying accidents and unusual behaviour [5]. This information can be fed to companies specialized in providing swift help in case of need, healthcare providers or concerned family members.

On-body or off-body sensors can be used for human activity monitoring in indoor environment. In the former category, triaxial accelerometers have been widely investigated for quantifying and classifying human activities [6]. The main drawback of on-body sensors is that these must be carried by the monitored subject at all times. In elderly care applications, where long monitoring periods are expected, subjects can be forgetful or uncooperative thus hampering the monitoring process. In the latter category, off-body sensing for movement analysis can be performed using technologies such as cameras [7], ultrasound [8] or pyroelectric infrared (PIR) sensors [9]. These approaches suffer however from limited range indoors as line of sight is usually constrained to a single room. The range limitation of these technologies means that many sensors are required to cover a single building. Furthermore, these multiple sensing units must be networked for data collection thus increasing the deployment and maintenance complexity of the system. Radar on the other hand is an attractive technology for long term monitoring of human movement because it does not need to be carried by the user, can be placed behind walls and is able to cover a large area depending on its operating parameters. Furthermore, the coarseness of the information provided by radars is less prone to raise privacy concerns when compared to cameras. Depending on the operating parameters, radars can also be used for through-the-wall sensing [10].

Deploying radars in health and wellness applications at the user's home will be facilitated if such systems are low cost, easy to deploy and safe. The possibility to adapt simple wireless LAN transceivers into indoor radars keeps the radar cost low and makes it flexible. Low radiation emission ensures safety for the user while multiple room coverage per radar unit eases deployment at home. However, extracting useful information from radars deployed in an indoor environment, where subjects may spend most or all their time, poses a challenge due to multipath propagation, presence of walls and other big objects, presence of interfering motions, etc. These properties of an indoor environment make it difficult to identify patterns of human movement from an indoor radar signal. Though these issues are addressed in this paper, the presence of interfering motions is not considered. In this work, a low-cost radar is designed that extracts human movement parameters in the presence of indoor multipath and clutter.

A radar signal reflected of a moving person carries rich information on his or her activity in the form a set of Doppler frequency patterns produced by the specific combination of limbs and torso movements. The Doppler frequency pattern that results from such a complex movement sequence is called "micro-Doppler signature" and the movement pattern is called "gait". If for a given activity, these Doppler signatures can be categorized into unambiguous profiles or "footprints", then radar signals can be used to identify the occurrence of specific activities over time. The evolution of these micro-Doppler patterns over time can be viewed in a spectrogram which is a time versus Doppler frequency plot of the micro-Doppler signatures. Spectrogram patterns obtained from human movement contain rich information on different parameters of movement including direction of motion, velocity, acceleration, displacement, cadence frequency, etc. Therefore, a visual inspection of spectrogram patterns reveals the occurrence of different types of human activities. However, to enable automatic human activity classification, parameters that have a unique range for the different types of human activities must be extracted from the micro-Doppler signature. Moreover, data storage and transmission of an entire spectrogram plot consumes too much storage and transmission resources. For efficient storage and transmission of human movement data to care taking centres, unique parameters that enable classification and require less transmission resources should be selected.

One of the most important parameters for the classification of human activities using Doppler signatures is the velocity profile [11], *i.e.*, the instantaneous velocity of human motion over time. Moreover, the velocity profile of a walking person shows different states (accelerate, decelerate, sudden stop, change in direction, etc.) that are useful to be identified in various applications. In general, a careful observation of how a person's velocity profile develops over time provides insights that can be used for timely intervention (if and when needed) in health and elderly care applications. Another important parameter for human activity classification is the rate of oscillation of the limbs which is called the "fundamental cadence frequency". This is an average rather than instantaneous parameter which shows how fast the legs and arms of a person are oscillating. The fundamental cadence frequency is an important parameter which can be directly utilized by an activity classification system [12], [11].

In this paper, different approaches to estimate these two important parameters of human motion, namely velocity profile and fundamental cadence frequency, are proposed and evaluated. The main contributions of this paper to the area of unobtrusive monitoring in health and wellness applications are as follows:

- Two different methods to estimate the velocity profile of human translational motion from the Doppler signature obtained in a form of time-frequency spectrogram are proposed and evaluated. The possibility of using high resolution Doppler spectrum estimation techniques is also introduced.
- A third simple method to estimate the velocity profile of

human motion based on phase difference computation is suggested and evaluated.

- An experimental radar platform based on low-cost software-defined radio hardware and open source software is implemented and its use for indoor monitoring of human movement is validated. The platform offers the opportunity of realizing low-cost experiments at an expedited pace and low budget.

The remainder of this paper is organized as follows: Section II reviews related work in the area of using radars for human activity monitoring, characterization and classification. Section III describes a human movement model that is crucial for the identification of the major Doppler components in the radar signal. Section IV introduces basic radar concepts in human sensing such as human radar cross-section and the radar signal model. Section V discusses the pre-processing and spectral estimation techniques that are relevant to obtain the micro-Doppler signatures. The proposed velocity profile and cadence frequency estimation methods are discussed in Sections VI and VII respectively. Section VIII describes the software defined radar platform and the experimental setup used in the validation experiments. The estimation results are presented and evaluated in Section IX. Finally, Section X summarizes and concludes the paper.

II. RELATED WORK

Human detection using radars has been extensively researched for military surveillance and rescue applications [13][14][10][15]. The use of radars for human activity monitoring and classification has also been intensively investigated. Anderson [16] used multiple frequency continuous wave radar for classification of humans, animals and vehicles. Otero [12] used a 10 GHz CW radar using micro-path antennas to collect data and to attempt classification. In addition [12] introduced a technique to estimate the cadence frequency of motion. Gurbuz et al. proposed a simulation based gender discrimination using spectrogram of radar signals [17]. Hornsteiner et al. applied radars to identify human motion [18]. Kim et al. used artificial neural network for classifying human activities based on micro-Doppler signatures [11]. All these papers used Fast Fourier Transform based frequency estimation.

There is also previous work on using other transforms for Doppler pattern estimation. Geisheimer et al. [19] introduced the chirplet transform as spectral analysis tool. The Hilbert-Huang Transform for non-linear and non-stationary signals in wide band noise radars is also suggested by Lay et al. [20]. A complex but more accurate iterative way to obtain each pixel in the spectrogram in a bid to improve the frequency resolution and suppress the side lobes of the Fast Fourier Transform is also suggested by Du et al. [21].

Even though the above authors have treated different aspects in human activity classification in general, the estimation of velocity profile in indoor environment where the received signal is plagued with multipath propagation was not specifically treated. Recently, spectrogram based methods to estimate the velocity profile of human walking were proposed in [1]. A

displacement estimation method based on computing phase difference is also proposed in [2].

In this paper, the spectrogram estimation methods in [1] are compared with another velocity profile estimation method derived from the phase difference principle in [2]. The use of sliding window high resolution parametric spectral estimator (MUSIC) is introduced and its performance for velocity profile estimation is compared with the commonly used Fast Fourier Transform. Moreover, a cadence frequency spectrogram is estimated and a simple method to estimate the fundamental cadence frequency from the spectrogram is suggested and evaluated.

III. HUMAN MOVEMENT MODEL

Our starting point for human activity characterization is the definition of a movement model. After studying the relationship between the different parts of the body during locomotion, features that have unique values in different activities can be identified. In this regard, the person's velocity profile is one of the important features that can be used to achieve activity classification.

The velocity profile refers to the instantaneous temporal displacement that the different parts of the human body attain during movement. Most of the human movement models available rely on dividing the non-rigid human body into the most significant rigid body parts and modelling the velocity profile of these rigid components. One of the most used human movement models [22] decomposes the body into 12 parts consisting of the torso, lower and upper part of each leg, lower and upper part of each arm, the head and each of the right and left foot. The torso is the main component or trunk of the body. This model also describes the kinematics of each of these body parts as a person walks with a particular velocity. Another known model was based on 3-D position analysis of reflective markers worn on the body using high resolution camera [23]. This model states that the velocity profile of each body part can be represented using low-order Fourier series. Using this model as a basis, we have described a modified human movement velocity profile as follows.

Assume a person is moving at a constant velocity V in a certain direction and that the human body consists of M rigid parts. The velocity profile of each part, $V_m(t)$, can be represented as a sum of sinusoids given by:

$$V_m(t) = V + A\{k_{m1} \sin(\omega_c t + p_m) + k_{m2} \cos(\omega_c t + p_m) + k_{m3} \sin(2\omega_c t + p_m) + k_{m4} \cos(2\omega_c t + p_m)\} \quad (1)$$

where $1 \leq m \leq M$. Note that the velocity profile of each body part V_m is characterized by amplitude constants: k_{m1}, \dots, k_{m4} and a phase constant: p_m ($0 \leq p_m \leq 180^\circ$). The oscillation amplitudes k_{m1}, \dots, k_{m4} are largest for legs and smallest for the torso. The phase p_m reflects the locomotion mechanism of the body. For instance, the right leg and left arm combination move 180° out of phase with respect to the left leg and right

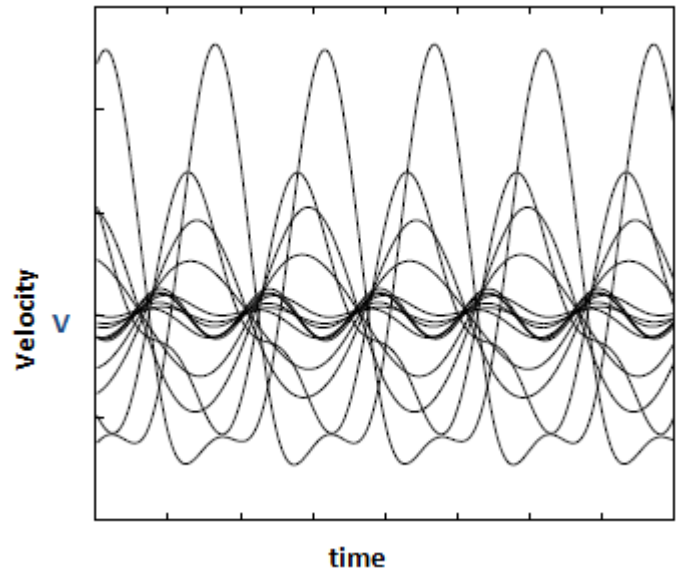


Figure 1. Human walking velocity profile model [18]

arm. A is a constant that has a specific value for different types of human activities, ω_c is the frequency of oscillation of the body parts which is also called the fundamental cadence frequency of motion.

A simulation of the velocity profile of a walking person based on a model similar to the one stated above is shown in Figure 1. As the Figure shows, the amplitude of oscillation of each body part is different; however, all the body parts oscillate at the same fundamental frequency ω_c and its second harmonics $2\omega_c$.

The translational velocity of the body is normally time-varying. Therefore, the oscillations of the body parts in (1) will be superimposed on the time varying velocity profile of the body. The torso has the smallest oscillation amplitudes, k_{m1}, \dots, k_{m4} and therefore the translational velocity profile V of the body can be approximated by the velocity of the torso. The translational velocity can thus be obtained by estimating the velocity of the torso. Therefore, the two terms: velocity profile of the body and velocity profile of the torso are assumed to be the same and used interchangeably from now on.

The velocity profile of the other parts of the body, $V_m(t)$ can thus be expressed as sinusoids superimposed on the velocity profile of the torso. Therefore, (1) can be expressed as:

$$V_m(t) = V_{torso}(t) + A\{k_{m1} \sin(\omega_c t + p_m) + k_{m2} \cos(\omega_c t + p_m) + k_{m3} \sin(2\omega_c t + p_m) + k_{m4} \cos(2\omega_c t + p_m)\} \quad (2)$$

IV. RADAR IN HUMAN SENSING

Radar is a device that transmits electromagnetic waves, receives the signal reflected back off the target and extracts information about the characteristics (range, velocity, shape, reflectivity, etc.) of the target. The amount of electromagnetic

energy that a target is capable of reflecting back is measured in terms of the radar cross section of the target. Doppler radars are those that measure the velocity of a target based on the Doppler effect, *i.e.*, an electromagnetic wave hitting a moving target undergoes a frequency shift proportional to the velocity of the target. The radar cross section and velocity profile are constant and easy to determine for a rigid body moving at a constant speed. However, as discussed in Section III, the human body locomotion is more complicated. The radar cross section and the signal model for radar based human movement monitoring are discussed in the following sections.

A. Human Body Radar Cross Section

Radar cross section (RCS) is a measure of signal reflectivity of an object and is usually expressed in a unit of area (e.g., m^2). RCS depends on the frequency of the transmitted signal and parameters of the target such as size, shape and material [24]. The RCS of a moving person is challenging to model because the human body is composed of multiple semi-independent moving parts. A simple additive approach to create an RCS model by adding up the contribution of each body part is commonly adopted. The contribution of each part can be assumed to remain constant during motion without significant error. In addition, the total RCS can be assumed to be half of the body surface area which is exposed when the person is facing the radar; this area is typically listed as $1m^2$ [25]. Each of the 12 major parts of the human body listed in Section III contribute to a fraction of the RCS. The torso has the highest RCS followed by the legs and arms. The head and feet have the least contribution. Particularly, the percentage contribution of each body part is listed as: torso 31%, arms 10% each, legs 16.5% each, head 9% and feet 7% [25].

As the torso has the highest RCS of all the moving body parts, the velocity profile of the torso can in principle be estimated by picking out the strongest component from the received Doppler signal.

B. Signal Model

Doppler radars measure the frequency shift of electromagnetic waves due to motion. The Doppler shift of an object is directly proportional to the velocity of the object and the carrier frequency of the transmitted signal as described below.

Assume a narrowband, unmodulated signal $a e^{j(2\pi ft + \phi_0)}$ is transmitted where a , f and ϕ_0 are the amplitude, carrier frequency and initial phase respectively. The signal received at the receiver antenna being reflected off a person has a time varying amplitude $a(t)$ and a time varying phase $\phi(t)$; thus it is given by $a(t) e^{j(2\pi ft + \phi_0 + \phi(t))}$. Hence, the received baseband signal after demodulation reduces to:

$$y(t) = a(t) e^{j\phi(t)} \quad (3)$$

The Doppler frequency shift, f_d is the rate of change of the phase of the signal, *i.e.*, $f_d(t) = -\frac{1}{2\pi} \cdot \frac{d\phi(t)}{dt}$ and a small change in phase can be expressed in terms of the change in distance as $\frac{d\phi(t)}{dt} = \frac{4\pi}{\lambda} \frac{dR(t)}{dt}$ where $R(t)$ represents the distance. This implies that the Doppler shift of a rigid target moving at a

velocity $V(t)$ is given by $f_d(t) = 2 \frac{V(t)}{\lambda}$ where λ is the wavelength of the transmitted radio wave and the velocity $V(t)$ represents $-\frac{dR(t)}{dt}$. This is in a mono-static radar configuration where the transmitter and receiver are co-located. In bi-static configuration where the transmitter and receiver are located on opposite sides of the target, the Doppler shift is given by $f_d(t) = \frac{V(t)}{\lambda}$.

It is stated in Section III that the different rigid components of the body have their own time-varying velocity profile superimposed on the body velocity. Therefore, each of these body parts have their own time-varying Doppler shift, *i.e.*, $f_{d_m}(t) = 2 \frac{V_m(t)}{\lambda}$ where $V_m(t)$ is the velocity profile of each body part. It is however generally challenging to extract the velocity profiles of each body part for the following reasons:

- The received signal is a superposition of signals that consist of Doppler shifts of different moving parts. Moreover, each body part has different RCS resulting in different contribution to the aggregate signal.
- There is significant multipath fading in indoor environment which results in further additive components to the resulting signal.
- A radar measures only the radial component of the velocity of the person, and thus only a portion of the movement can be estimated with signals from a single radar.

The content that follows emphasizes on how to estimate the velocity profile of the body from the aggregate received signal.

A typical walking of a person in an indoor environment is described by non-uniform motion, *i.e.*, the velocity profile of the body varies with time. However, physical constraints limit the person from changing velocity during very short time intervals. Consequently, the person's velocity can be assumed to remain constant during short time intervals. In other words, a non-uniform human motion can be viewed as a uniform motion over small time or displacement intervals. This corresponds to the idea that the non-stationary radar signal received as a reflection from the person can be assumed to be piece-wise stationary. Based on this argument, the received signal during a small piece-wise stationary interval can be assumed to be a summation of a certain number of sinusoids. If D sinusoids are assumed, the received signal after sampling can be given by:

$$y[n] = \sum_{d=1}^D \left[a_d \cdot e^{j\left(\frac{4\pi V_d[n]T}{\lambda} n + \phi_d\right)} \right] \quad (4)$$

where $y[n]$ is a sample at time instant nT , T is the sampling time and a_d , V_d and ϕ_d are respectively the amplitude (which is proportional to the RCS), velocity and initial phase of each Doppler frequency component. Since the amplitude undergoes large scale variations as compared to the phase which varies from sample to sample, here it is assumed that the amplitude a_d is not time varying in the piece-wise stationary interval.

The indoor environment consists of stationary objects such as walls that have larger RCS than the human body. The

signal reflected from these stationary objects has zero Doppler frequency shift. Moreover, there is a strong direct signal between the transmitter and receiver antennas of the radar. The resulting effect is a strong DC component in the baseband radar signal. Therefore, the received radar signal is actually given by:

$$y[n] = a \cdot e^{j\phi} + \sum_{d=1}^D \left[a_d \cdot e^{j\left(\frac{4\pi V_d [n] T}{\lambda} n + \phi_d\right)} \right] \quad (5)$$

The number of sinusoids D may change between consecutive intervals, but it is assumed to remain constant to avoid complexity. The value of D can be taken as small as the number of body parts described in Section III; however, it is generally better to assign it a larger number to obtain a smooth Doppler spectrum pattern.

V. DOPPLER SPECTRUM ESTIMATION

The received radar signal consists of many frequency components as described in the previous section. If piecewise stationarity is assumed, a joint time-frequency estimation can be used to decompose the received signal into these frequency components. In order to estimate the spectral content of a signal, non-parametric or parametric spectral estimators can be applied [26]. In this work, the Short Time Fourier Transform (STFT) and a high resolution parametric estimator, sliding window Multiple Signal Classification (MUSIC) are used. However, as discussed in Section IV-B, the zero-frequency component which results due to stationary objects in the environment must be removed before spectrum estimation.

A. Pre-processing

As shown in (5), there is a strong DC component in the aggregate received signal. This component contains no information and makes the spectral magnitudes of the other relevant frequencies almost invisible in the spectrogram. Moreover, it affects estimation of the relevant Doppler frequency patterns which have small amplitudes. Therefore, this component must be removed for better estimation.

There are different techniques to eliminate a DC component from a signal. The simplest method available is adopted here, *i.e.*, averaging. The average value of the signal is computed and subtracted from the aggregate signal as follows:

$$\hat{y}[n] = y[n] - \frac{1}{N_{av}} \sum_{n=1}^{N_{av}} y[n] \quad (6)$$

where N_{av} is a large number. The remaining signal $\hat{y}[n]$ can be thus assumed to consist of the useful Doppler frequency pattern from moving objects only.

B. Spectrum Estimation

The short time Fourier transform (STFT) applied on the signal, $\hat{y}[n]$ is given by:

$$Y[k, n'] = \sum_{n=n'}^{n'+L} \hat{y}[n] \cdot e^{-j2\pi nk/N} \quad (7)$$

where L is the number of signal samples taken in each consecutive computation which is called "window size" in spectral estimation; n' , which is set to multiples of $(1 - \alpha)L$, represents the starting points of the moving window transform and α is the overlap factor between windows. k represents the k^{th} frequency component of the signal, and N is the size of the FFT. The window size L is set based on the duration over which the signal is assumed stationary. This form of short time FFT computation is also called sliding window FFT.

For the sake of comparison, a MUSIC [26] based spectral estimation is also applied to the received signal. MUSIC is a parametric spectral estimator based on eigenvalue decomposition. Sliding window MUSIC based spectral estimation is not commonly used; however, it is intuitive that it can be applied similar to the sliding window FFT. In the STFT, the window size is a trade-off between stationarity and spectral resolution. The major advantage of parametric spectral estimators like MUSIC is that the spectral resolution is independent of the window size L . However, the MUSIC method requires a priori knowledge of two parameters: the auto-correlation lag parameter and the number of sinusoids D [26]. The performance of the MUSIC method can be better or worse than STFT based on the setting of these two parameters.

The joint time-frequency spectral estimation is represented using the spectrogram, a color plot of the magnitude of frequency components as a function of time and frequency. The pixels in the spectrogram represent the power at a particular frequency and time, which is computed as: $P[k, n'] = |Y[k, n']|^2$.

VI. VELOCITY PROFILE ESTIMATION METHODS

As discussed in Section III, each body part has its own velocity profile superimposed on the velocity profile of the torso. The instantaneous torso velocity $v_{torso}[n']$ can be obtained from the instantaneous torso Doppler frequency $f_{torso}[n']$ using:

$$v_{torso}[n'] = \frac{\lambda}{2} f_{torso}[n'] \quad (8)$$

Three methods to estimate the velocity profile of human walking are suggested. The first two methods are based on the the joint time-frequency estimation discussed in Section V. The torso Doppler frequency profile is estimated using these two methods and the corresponding velocity profile is obtained using (8). The third method is different from the two methods. It is a simple but approximation-based method based on phase difference computation.

A. Maximum Power Method

As described in Section III, the torso has the largest RCS of all the body parts. Thus, the frequency component which has the highest power must be the Doppler frequency component of the torso since the strongest DC component is already removed. The maximum power method selects the frequency of maximum power from each spectral window in the computed

spectrogram, i.e., $f_{torso}[n'] = f[k_{torso}, n']$, where k_{torso} is the frequency index at which $P[k, n']$ is maximum.

However, selecting the maximum frequency component returns the torso frequency component only when there is motion. If there is no motion, the received signal $\hat{y}[n]$ in (6) consists of only background noise and therefore selecting the strongest frequency component gives a wrong estimate of the torso frequency (which is actually zero). A threshold parameter must thus be selected to distinguish motion and no-motion intervals (for instance, in Figure 4, the interval of no-motion is 0-3 s). This parameter will be computed from the signal received when there is no motion and used as a threshold. The total signal power in the spectrogram column is one of the suitable parameters that can be used to distinguish these intervals. The parameter is computed and averaged over the duration of no-motion to determine a threshold, i.e., $P_{thr} = average_{n'}\{\sum_{k=1}^N P[k, n']\}$. Therefore,

$$f_{torso}[n'] = \begin{cases} f[k_{torso}, n'] & \text{if } \sum_{k=1}^N P[k, n'] > P_{thr} \\ 0 & \text{else} \end{cases} \quad (9)$$

B. Weighted Power Method

The maximum power method requires a threshold which may fail to distinguish the motion and no-motion intervals correctly. This can result in a non-zero velocity estimate in absence of motion or zero velocity even though there is motion. Thus a method that pulls the velocity to zero when there is no or little motion without using a threshold is desirable. This method should also pull the resulting velocity estimate to torso velocity when there is motion.

One possible way to do this is to estimate $f_{torso}[n']$ as a power-weighted average frequency in each spectrogram column, n' , i.e.,

$$f_{torso}[n'] = \frac{\sum_{k=1}^N f[k, n'] \cdot P[k, n']}{\sum_{k=1}^N P[k, n']} \quad (10)$$

This is based on the assumption that the frequency index range considered in the spectrogram is $[-Fs/2 : Fs/2]$ (where $Fs = \frac{1}{T}$ is the sampling frequency) or the zero frequency is the central point in the spectrogram.

The major problem of the weighted power method is that it results in a biased estimate when image frequencies are present. Image frequencies are those Doppler frequencies that occur on the opposite side of the actual Doppler frequency pattern in the spectrogram. These occur due to multipath effect in indoor environments. For instance, when a person is moving towards the radar, the Doppler frequencies are positive. However, there are also signals that reflect on the back of the person and received in the aggregate signal. As the person is moving away from the radar with respect to these signal paths, the signal components create negative (image) frequencies. The presence of image frequencies makes the weighted power estimate biased with respect to the actual torso frequency. However, the rays that reflect off the back of the person travel longer distances as compared to the rays that reflect off the front of the person and therefore, these

components have lower power levels. The low power level of image frequencies reduces their impact on the weighted power.

The maximum power method is not affected by the presence of image frequencies as it simply selects the strongest frequency component. The weighted power method however performs well even in static conditions and is easier to apply as there is no need for a threshold.

C. Phase Difference Method

The third instantaneous velocity estimation method is derived from the total displacement estimation method suggested in [2] which was based on phase difference computation. In narrowband signals, the change in phase can be directly related to the propagation delay. Therefore, the change in phase can be directly related to the change in distance or the change in distance per unit time which is the instantaneous velocity.

After removing the DC component using (6), the received signal in (5) can be expressed as:

$$\hat{y}[n] = \sum_{d=1}^D \left[a_d \cdot e^{j\left(\frac{4\pi V_d [n] T}{\lambda} n + \phi_d\right)} \right] \quad (11)$$

Lets make a crude approximation that there is only one strong reflection in the received signal and all the other reflections are very weak. It is mentioned that if there is one strong component in the reflection from the human body, that strong component is the reflection from the torso. Using this assumption, (11) reduces to:

$$\hat{y}[n] \approx a_{torso} \cdot e^{j\left(4\pi V_{torso}[n] \frac{T}{\lambda} n + \phi_d\right)} \quad (12)$$

The instantaneous torso velocity can be easily be obtained from (12) by computing the phase difference between consecutive samples. The phase difference between consecutive samples $\Delta\phi[n]$ can be computed by:

$$\Delta\phi[n] = \angle(\hat{y}[n]\hat{y}^*[n-1]) \approx 4\pi V_{torso}[n] \frac{T}{\lambda} \quad (13)$$

This change in phase $\Delta\phi[n]$ should be very small here ($\Delta\phi[n] \ll 2\pi$) to avoid phase ambiguity. However, this is not a problem for typical sampling rates of a few hundred Hz and radar transmission frequencies less than 10 GHz which is also the case in our software radio-based radar.

Therefore, the torso velocity can be obtained as:

$$V_{torso}[n] \approx \Delta\phi[n] \frac{\lambda}{4\pi T} \quad (14)$$

It is discussed that human motion is piece-wise stationary; thus, a resolution more than a fraction of a second is not necessary. The motion is assumed to be stationary over L samples for spectrum estimation in Section V-B. Using a similar piece-wise stationarity range of L , the velocity profile of the torso is thus given by:

$$V_{torso}[n'] \approx \frac{\lambda}{4\pi LT} \sum_{n=n'}^{n'+L} \Delta\phi[n] \quad (15)$$

Besides estimating the velocity profile at an appropriate interval, the averaging in (15) has the advantage of averaging out the noise when there is no motion. Assuming that the noise is additive white noise when there is no motion (when the velocity is zero), the summation in (15) tends to zero. Therefore, a near zero torso velocity ($V_{torso}[n'] \approx 0$) is obtained.

The phase difference method is therefore a very simple method that can be used to estimate the velocity profile of human motion with less complexity. It is a simple method because the complexity associated with spectrogram estimation and the task of extracting the velocity profile from the spectrogram are avoided.

However, the phase difference method has its own drawbacks. The first drawback is its accuracy. As already mentioned, the phase difference method is dependent on the crude assumption that the reflection from the torso is the only significant reflection in the received signal. Therefore, the accuracy of this method is dependent on the ratio of the magnitude of the signal reflection from the torso to the magnitude of the aggregate received signal. The smaller this ratio, the less accurate the method will be. A detailed illustration on the accuracy of this phase difference computation is given in [2]. The second drawback of this method is that it gives inaccurate results when the background noise (the signal received when there is no motion) is not white. Such a coloured background signal may result from harmonics and other frequency components generated by imperfect transceivers. In presence of a coloured noise, the phase difference method gives a velocity estimate corresponding to the strongest background noise frequency. Therefore, unless background subtraction methods as suggested in [2] are used, the phase difference method does not estimate the velocity profile correctly in the absence of motion.

VII. CADENCE FREQUENCY ESTIMATION

Cadence frequency is an important parameter of motion that shows how fast the appendages (legs and arms) of the body are oscillating. A cadence frequency spectrum shows the rate of change of each Doppler frequency: whether the magnitude of a particular Doppler frequency has a constant strength over time or has a certain rate of change. For instance, the torso has near to constant velocity (does not oscillate) as compared to the hands and legs whose velocity changes continuously in an oscillatory pattern. Such a pattern can be obtained from a cadence frequency spectrogram.

A cadence frequency spectrogram can be obtained by taking the FFT of the Doppler frequency versus time spectrogram over time at each Doppler frequency. Thus, the Doppler frequency versus time plot will be transformed into Doppler frequency versus cadence frequency plot. That is, the power of the signal $P_c[k, c]$ at a Doppler frequency index k and cadence frequency index c is given by:

$$P_c[k, c] = \left| \sum_{n'=1}^{N_w} |Y[k, n']| e^{-j \frac{2\pi}{N_w} cn'} \right|^2 \quad (16)$$

where $Y[k, n']$ is given by (7). The number of time windows involved in the FFT, N_w , should be short enough to estimate the change in cadence frequency pattern, *i.e.* to have enough time resolution, and it should be long enough to get enough cadence frequency resolution. Thus, an optimal window size should be taken considering these factors. The maximum cadence frequency to be considered depends on the time interval between consecutive windows.

Once the cadence frequency spectrogram is obtained, a simple method of summing the total power at each cadence frequency can be used to obtain the fundamental cadence frequency of the gait. Summing the powers at each cadence frequency over the Doppler bins gives a total power versus cadence frequency plot. The total power at a cadence frequency index c , $P_t[c]$, is thus given by:

$$P_t[c] = \sum_{k=1}^N P[k, c] \quad (17)$$

Based on the velocity profile model in (1), three peaks are expected on the cadence frequency plot. The first and strongest peak will be at a cadence frequency of 0 due to the near constant velocity of the torso, the second peak will be at the fundamental frequency ω_c and the third at the second harmonics $2\omega_c$. More harmonics orders might also be visible from the spectrogram. Therefore, the second peak from the cadence frequency plot is taken as the fundamental cadence of the gait.

VIII. SOFTWARE RADIO-BASED RADAR

The velocity profile and cadence frequency estimation methods discussed were evaluated in a set of experiments done using a GNU Radio-based active radar.

GNU Radio is an open source and free programming toolkit used for realizing software defined radios using readily-available, low-cost RF hardware and general purpose processors [27], [28]. The toolkit consists of a variety of signal processing blocks implemented in C++ that can be connected together using Python programming language. Some of the nice features of GNU Radio include the fact that it is free, open-source, re-configurable, can tune parameters in real-time and provides data flow abstraction. The Universal Software Radio Peripheral (USRP) is a general purpose programmable hardware that is commonly used as a front-end for GNU Radio [29].

The major components of the USRP are its FPGA, ADC/DAC sections and interpolating/decimating filters. The USRP is designed such that the high sampling rate signal processing, such as down conversion, up conversion, decimation, interpolation and filtering are done in the FPGA. The low speed signal processing such as symbol modulation/ demodulation, estimation and further signal processing takes place in the host processor. This lessens computational burden of the processor and makes signal processing easily manageable. The new USRP version, USRP2, has a Gigabit Ethernet interface

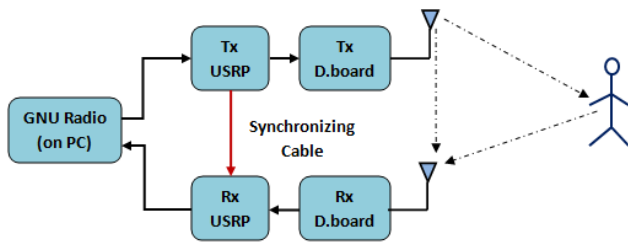


Figure 2. Monostatic radar setup using GNU Radio and USRP

allowing 25 MHz RF bandwidth in and out of the USRP2 [27], [30].

GNU Radio and USRP have been widely used for prototyping in communication systems research [27]. Their adoption in a wide range of applications is motivated by the low cost, relative ease to use and flexibility. However, the use of USRP as a platform for building active radar is limited due to its low power and limited bandwidth. A possible design of USRP based long-range pulse radar is discussed in [31]. We instead used a USRP based continuous wave radar. To the best of our knowledge, our work is the first using USRP and GNU Radio as a short-range (indoor) active radar.

In our experiments, a USRP is used in conjunction with GNU Radio to implement a monostatic, unmodulated continuous wave radar. The USRP was equipped with a XCVR2450 daughterboard which works as the radar RF front-end in the $2.4 - 2.5$ and $4.9 - 5.9\text{ GHz}$ bands. Figure 2 shows the schematics of our radar. The setup uses two separate USRPs, one for transmission and the other dedicated for reception. A cable between the boards ensures the two boards are synchronized to a common clock.

This radar platform is both low-cost and flexible. The carrier frequency, transmitter power, receiver gain, and other parameters are easily configurable in software.

IX. EVALUATION

A detailed description of the different types of experiments done and the results obtained to evaluate the estimation of human movement parameters such as velocity profile, cadence frequency, displacement, activity index, direction of motion, etc., can be found in [32]. In this paper, only one of the experiments to evaluate the proposed velocity profile and cadence frequency estimation methods is described.

In the evaluation experiment, a person's movement in a confined area was measured using radar transmission frequency of 5 GHz and transmission power of 30 dBm (including antenna gains). The received signals were recorded in a data file and processed offline using MATLAB. The signal was low-pass filtered and decimated to a sampling rate F_s of 500 S/s . A window size of 100 samples which corresponds to 0.2 s (where s represents seconds) is used assuming that the motion is piece-wise constant for a time duration of 0.2 s . An FFT size (N) of 500 and an overlap of 75% between the sliding windows are also used in the computation of both STFT

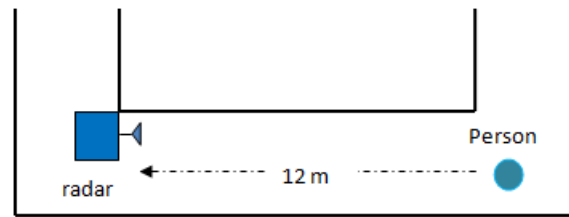


Figure 3. Walking experiment made in a corridor

and MUSIC spectrograms. In MUSIC, the autocorrelation lag parameter is set to $0.5L$ and the number of sinusoids D is set to 25. Such a value of D was chosen after experimenting on the received signal and taking into account the discussion in Section IV.

Some important parameters of motion that can be easily observed from the spectrogram are discussed and compared with the actual motion of the subject. The velocity profile is estimated using the three methods discussed in Section VI. These velocity estimation methods are evaluated by computing the total distance covered based on the velocity profile estimated and comparing it with the actual distance covered by the subject which was measured manually. The weighted mean method is then selected to estimate and compare velocity estimations from the STFT and MUSIC based spectrograms. The number of steps taken to complete the motion are also recorded and used to evaluate the fundamental cadence frequency estimation method discussed in Section VII.

The experiment was done in a 2 m wide and 12 m long corridor as shown in Figure 3. The person stands at a distance of 12 m in front of the radar for about 3 s and starts walking towards the radar. Measurements with a timer and manual counting showed that it takes the person about 10 s and 15 walking steps respectively to complete the 12 m by walking.

A. Spectrograms

The STFT and MUSIC based spectrograms obtained from this experiment are shown in Figure 4 and 5 respectively. These spectrograms show the micro-Doppler pattern of the motion of the person over time. The following observations can be derived from these spectrograms:

- The time duration of motion recorded and the number of steps counted manually match the spectrogram pattern. The latter, which is counted to be 15 during the experiment, is equal to the number of spikes in the spectrogram (which is also 15 as Figure 4 shows more clearly). These spikes result from the forward swinging of the legs and arms. The periodic like pattern of the spikes in the spectrogram corresponds to the oscillation of the legs and arms that occur in a typical walking sequence. The spectrogram also shows that the backward swinging of the legs is small as compared to the forward swinging. This confirms the asymmetrical human movement model patterns observed in Figure 1.

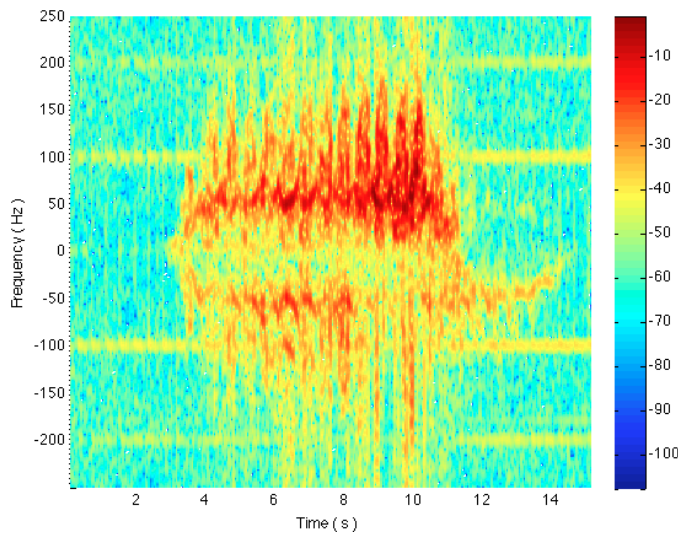


Figure 4. STFT based spectrogram estimate

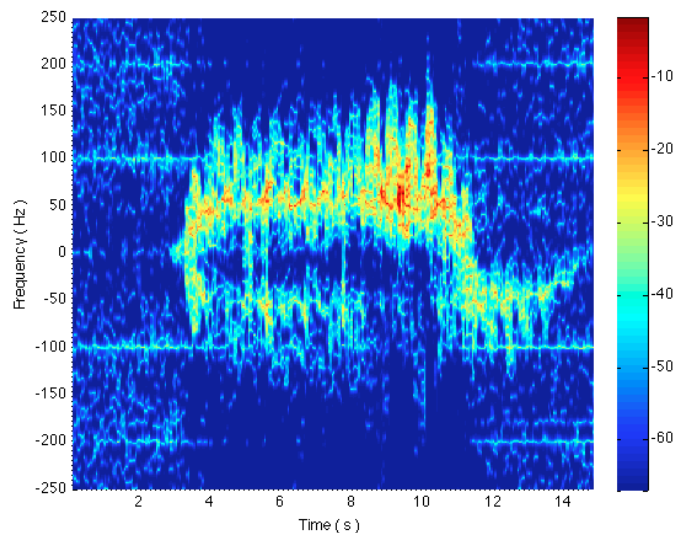


Figure 5. MUSIC based spectrogram estimate

- Even though the person is moving towards the radar which corresponds to a positive Doppler frequency, the spectrograms shows that there is an image micro-Doppler pattern of weaker power level in the negative Doppler frequencies. This confirms the image frequency problem discussed in Section VI.
- The STFT spectrogram has lower resolution than the MUSIC spectrogram as expected. On the other hand, the STFT micro-Doppler pattern is smooth as compared to a spiky MUSIC spectrogram that resolves the strongest frequencies as Figure 5 shows. Therefore, it can be deduced that the MUSIC spectrogram can be used to resolve the specific Doppler contribution of each of the rigid parts of the body.

B. Velocity Profile

The torso velocity profile estimated using the two spectrogram based velocity estimation methods, namely maximum power and weighted power methods, is shown in Figure 6. These estimates are based on the STFT spectrogram in figure 4. The performance of the phase difference method is also plotted in Figure 7 in comparison to the spectrogram based methods. The following can be said on the performance of these velocity profile estimation methods.

One possible measure to evaluate the accuracy of these methods is the total distance covered. This measure can only test the accuracy of the velocity profile estimations in average. To measure the total distance, a part of the spectrogram when the person is in motion must be considered (which is between 3 s and 11 s as shown in Figure 4). The total distance the person moved can then be estimated as the area under the velocity versus time curve. That is, Total distance = $8 s \cdot \sum_{t=3s}^{11s} V_{torso} [t]$. A total distance of 13.26 m is obtained from the maximum power method which gives an error percentage of only 10% as compared to the manually measured distance of the corridor which is 12 m. Similarly, a total distance of 11.34 m is obtained from the weighted mean method which gives an error percentage of only 5.5%. The total distance computed from the phase difference method is about 12.85 m which results in an error percentage of 7%. These results show that all velocity profile estimation methods estimate the total distance with an error of less than 10% and the weighted mean method gives the best estimate.

The other measure that can be used is the performance of these methods when there is no motion (which is between 0 s and 3 s as shown in Figure 4). As Figure 7 shows, the maximum power method is able to perform well (outputs $V_{torso}[n'] = 0$) in absence of motion since it uses a threshold detector. On the other hand, the weighted power and phase difference methods have a significant error in the absence of motion. The figure shows that the phase difference method has the worst performance in the absence of motion due to the imperfect transceivers as discussed in Section VI-C. The background noise frequencies generated by our software radio-based radar prototype are evident from the horizontal symmetrical lines at 100 Hz and 200 Hz in Figure 4.

One of the nice properties of the weighted power method is that it is insensitive to symmetrical background noise. Therefore, the weighted power method has in average better accuracy than the phase difference and maximum power methods.

STFT versus MUSIC: The spectrograms in Figure 4 and 5 show that MUSIC is a good spectral estimator to resolve the contribution of the rigid parts of the body from the overall micro-Doppler signature. In order to evaluate the accuracy of velocity estimations computed from STFT and MUSIC spectrograms, the weighted power method is used. A comparative plot of the velocity estimations based on an STFT and MUSIC spectrogram is shown in Figure 8 for the duration of motion.

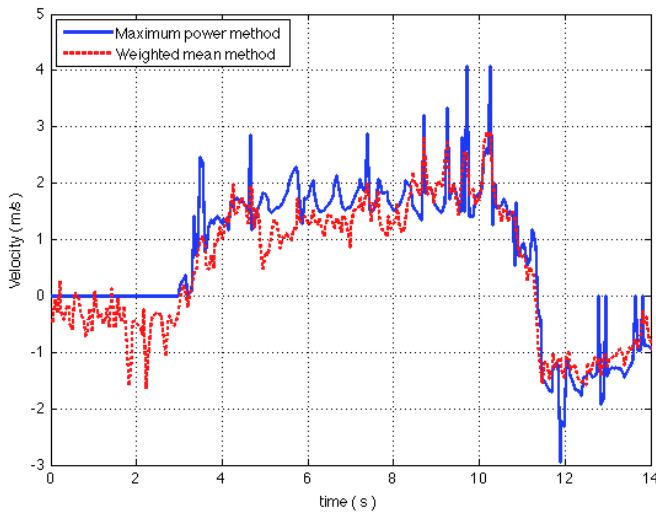


Figure 6. Spectrogram based velocity profile estimation methods

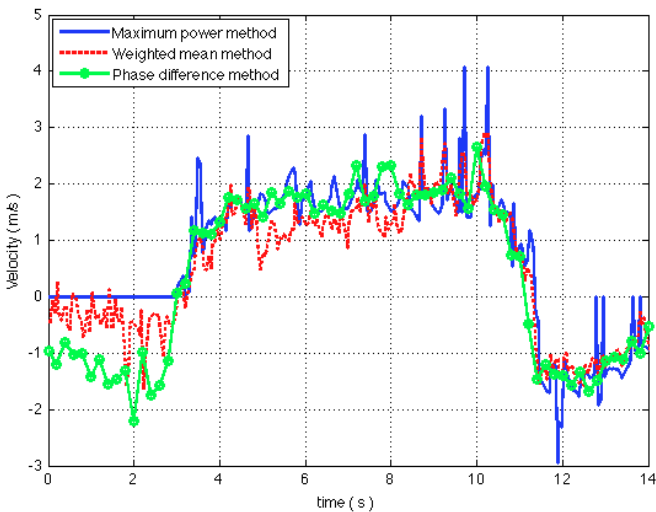


Figure 7. Phase difference method of velocity profile estimation compared with the spectrogram based estimates

The total distance is computed from these velocity estimations and is found to be 11.34 m (estimation error of 5.5%) for the STFT based spectrogram and 12.34 m (estimation error of 2.83%) for the MUSIC based spectrogram. This result suggests that the MUSIC based method outperforms the STFT based method in average. However, there is no significant difference between the two velocity profiles as Figure 8 shows. This is because the estimation methods in Section VI are not very sensitive to frequency resolution.

C. Cadence Frequency

The cadence frequency spectrogram can be obtained from the STFT or MUSIC spectrograms by applying Fourier transform at each Doppler frequency as discussed in Section VII. In this case the STFT spectrogram is used.

The cadence frequency spectrum obtained from the STFT spectrogram is shown in Figure 9. This spectrum shows the

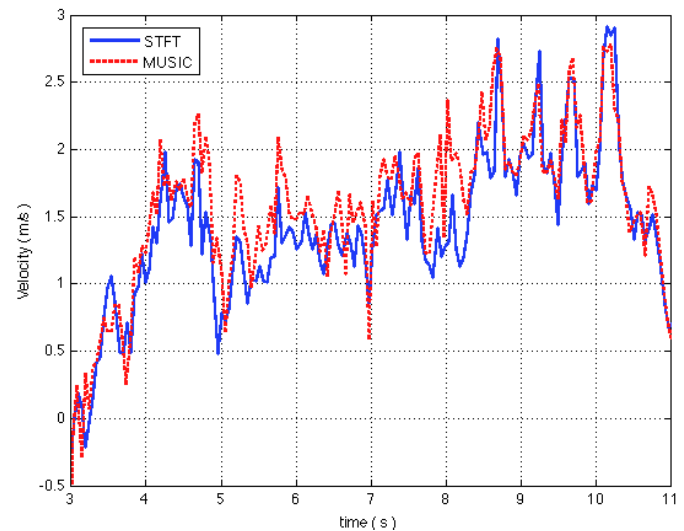


Figure 8. Velocity profile estimates using STFT and MUSIC based spectrograms

Doppler frequencies and their corresponding rate of oscillation contributed by the parts of the body. Small cadence frequency corresponds to no oscillation or variation of a Doppler component and large cadence shows high rate of oscillation. As indicated, the strongest Doppler frequency at zero cadence corresponds to the torso and the other strongest component at a higher cadence (which is the fundamental cadence of the gait) corresponds to the legs.

In order to obtain the fundamental cadence of the gait, the total power at each cadence frequency bin is summed and plotted as shown in Figure 10. This figure clearly shows two strongest cadence frequencies. It is evident from the human movement model in Section III that three strongest frequencies: 0, ω_c and $2\omega_c$ are expected from the cadence frequency plot. However, the second cadence is found to be weak here.

The fundamental cadence frequency (the second peak) is obtained from Figure 10 to be 1.74 steps/s. This parameter shows how many walking steps the person makes per second in average. As discussed in Section I, this parameter indicates the activity level and possibly the health status of a person. The cadence frequency estimation can be verified based on the manually recorded data when the experiment is done. It is stated that the number of steps the person took to cover the distance is 15 and the duration of motion as observed from the spectrograms to be 8 s. Therefore, the fundamental cadence frequency is $\frac{15 \text{ steps}}{8 \text{ s}} = 1.87 \text{ steps/s}$ which shows that the estimation results in an error of 6.9% only.

X. CONCLUSION

In this paper, pre-processing followed by STFT and MUSIC spectral estimators are applied to estimate the micro-Doppler signatures of human movement from a received radar signal. Elegant approaches to estimate the velocity profile and fundamental cadence frequency of motion are proposed.

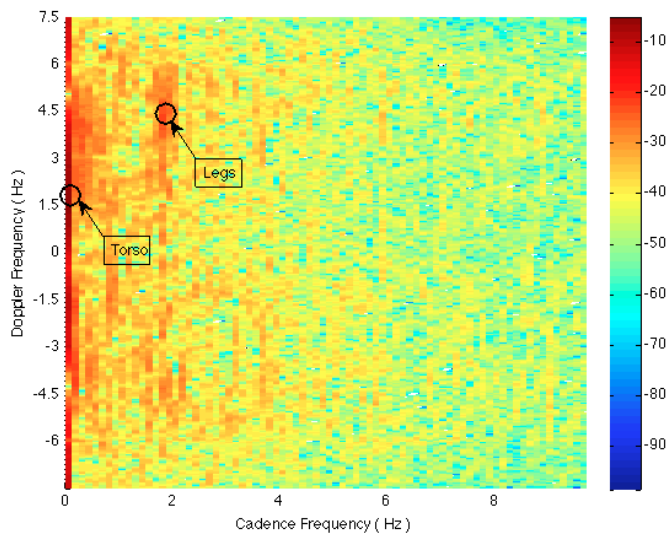


Figure 9. Cadence frequency spectrogram

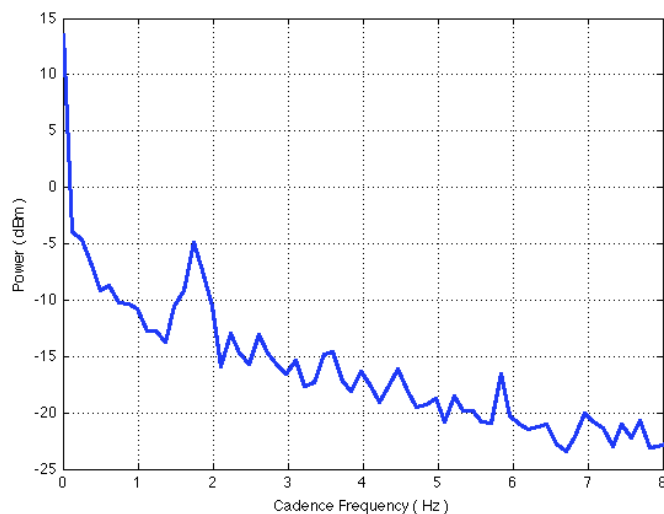


Figure 10. Total power versus cadence frequency showing the peak at the fundamental cadence frequency

Maximum power and weighted mean methods are suggested to extract the velocity profile from the spectrograms as well as an approximate but simple method based on phase difference computation. These velocity profile estimation methods are evaluated and compared against each other. A technique to extract the cadence frequency spectrum and the fundamental cadence frequency from the joint time-frequency estimation is also discussed and evaluated.

The maximum power, weighed mean and phase difference methods were able to measure the total distance covered with an error of 10%, 5.5% and 7% respectively. It is found that the maximum power method is error-prone since it needs a threshold and its performance depends on the choice and accurate estimation of the threshold value. The phase difference method is found to be accurate enough in the presence of motion. However, the sensitivity of this method to background

noise makes it error-prone in the absence of motion. In weak image frequencies (outdoor environment for instance), the weighted power method is a suitable method. Its insensitivity to symmetrical coloured background noise is also another factor that makes the weighted mean method attractive. It can be concluded that the weighted power method outperforms both the maximum power and phase difference methods in average. However, the maximum power method is preferable in presence of strong image frequencies.

It is also shown that the MUSIC based spectrogram not only provides a resolved spectrogram showing the contribution of each component but also results in a smaller velocity profile estimation error. It is also found that the fundamental cadence frequency is estimated with an error of less than 7%. In general, it can be concluded that all velocity estimation methods suggested are able to estimate the velocity profile of human translational motion with an accuracy that is good enough for the applications concerned.

A major limitation of the velocity estimation methods discussed so far is that only the radial component of the velocity is being perceived and estimated by the radar. One way to achieve a better estimation is by combining information from two or more radars adjusted to monitor distinct directions. In addition, the velocity estimation methods discussed in this paper do not consider the possible presence of other interfering motions and assume that there is a single mover in the monitored environment. In applications where this is not acceptable, it is essential to be able to discriminate and track the velocity profiles of multi-movers. Research on extracting the velocity profile of multi-movers in indoor environment is considered in future work.

REFERENCES

- [1] B. Godana, G. Leus, and A. Barroso, "Estimating indoor walking velocity profile using a software radio-based radar," in *Sensor Device Technologies and Applications (SENSORDEVICES), 2010 First International Conference on*, pp. 44–51, 2010.
- [2] B. Godana, G. Leus, and A. Barroso, "Quantifying human indoor activity using a software radio-based radar," in *Sensor Device Technologies and Applications (SENSORDEVICES), 2010 First International Conference on*, pp. 38–43, 2010.
- [3] B. de Silva, A. Natarajan, M. Motani, and K.-C. Chua, "A real-time exercise feedback utility with body sensor networks," in *5th International Summer School and Symposium on Medical Devices and Biosensors, ISSS-MDBS 2008.*, pp. 49–52, June 2008.
- [4] B. Lo, L. Atallah, O. Aziz, M. E. Elhew, A. Darzi, and G. zhong Yang, "Real-time pervasive monitoring for postoperative care," in *4th International Workshop on Wearable and Implantable Body Sensor Networks, BSN 2007*, pp. 122–127, 2007.
- [5] S.-W. Lee, Y.-J. Kim, G.-S. Lee, B.-O. Cho, and N.-H. Lee, "A remote behavioral monitoring system for elders living alone," in *International Conference on Control, Automation and Systems, ICCAS '07.*, pp. 2725–2730, Oct. 2007.
- [6] A. Purwar, D. D. Jeong, and W. Y. Chung, "Activity monitoring from real-time triaxial accelerometer data using sensor network," in *International Conference on Control, Automation and Systems, ICCAS '07.*, pp. 2402–2406, Oct. 2007.
- [7] Z. Zhou, X. Chen, Y.-C. Chung, Z. He, T. Han, and J. Keller, "Video-based activity monitoring for indoor environments," in *IEEE International Symposium on Circuits and Systems, ISCAS 2009.*, pp. 1449–1452, May 2009.
- [8] Y. Tsutsui, Y. Sakata, T. Tanaka, S. Kaneko, and M. Feng, "Human joint movement recognition by using ultrasound echo based on test feature classifier," in *IEEE Sensors*, pp. 1205–1208, Oct. 2007.

- [9] S.-W. Lee, Y.-J. Kim, G.-S. Lee, B.-O. Cho, and N.-H. Lee, "A remote behavioral monitoring system for elders living alone," in *International Conference on Control, Automation and Systems, ICCAS '07.*, pp. 2725–2730, Oct. 2007.
- [10] R. M. Narayanan, "Through wall radar imaging using UWB noise waveforms," in *Proc. IEEE International Conference on Acoustics, Speech and Signal Processing ICASSP 2008*, pp. 5185–5188, Mar. 2008.
- [11] Y. Kim and H. Ling, "Human activity classification based on micro-Doppler signatures using an artificial neural network," in *IEEE Antennas and Propagation Society International Symposium, AP-S 2008*, pp. 1–4, July 2008.
- [12] M. Otero, "Application of continuous wave radar for human gait recognition," in *Proc. SPIE*, vol. 5788, pp. 538–548, 2005.
- [13] H. Burchett, "Advances in through wall Radar for search, rescue and security applications," in *Proc. Institution of Engineering and Technology Conference on Crime and Security*, pp. 511–525, June 13–14, 2006.
- [14] D. J. Daniels, P. Curtis, and N. Hunt, "A high performance time domain UWB Radar design," in *Proc. IET Seminar on Wideband Receivers and Components*, pp. 1–4, May 7–7, 2008.
- [15] S. S. Ram, Y. Li, A. Lin, and H. Ling, "Doppler-based detection and tracking of humans in indoor environments," *Journal of the Franklin Institute*, vol. 345, pp. 679–699, 2008.
- [16] M. G. Anderson, *Design of multiple frequency continuous wave radar hardware and micro-Doppler based detection and classification algorithms*. PhD thesis, University of Texas, Austin, May 2008.
- [17] S. Gurbuz, W. Melvin, and D. Williams, "Detection and identification of human targets in Radar data," in *Proc. of SPIE Defense and Security Symposium*, 2007.
- [18] C. Hornsteiner and J. Detlefsen, "Characterisation of human gait using a continuous-wave Radar at 24 GHz," *Advances in Radio Science*, vol. 6, pp. 67–70, 2008.
- [19] J. Geisheimer, W. Marshall, and E. Greneker, "A continuous-wave (CW) radar for gait analysis," in *Thirty-Fifth Asilomar Conference on Signals, Systems and Computers*, vol. 1, pp. 834–838 vol.1, 2001.
- [20] C.-P. Lai, Q. Ruan, and R. M. Narayanan, "Hilbert-Huang transform (HHT) processing of through-wall noise radar data for human activity characterization," in *IEEE Workshop on Signal Processing Applications for Public Security and Forensics, SAFE'07*, pp. 1–6, April 2007.
- [21] L. Du, J. Li, P. Stoica, H. Ling, and S. Ram, "Doppler spectrogram analysis of human gait via iterative adaptive approach," *Electronics Letters*, vol. 45, pp. 186–188, 29 2009.
- [22] R. Boulic, N. Magnenat-thalmann, and D. Thalmann, "A global human walking model with real-time kinematic personification," *The Visual Computer*, vol. 6, pp. 344–358, 1990.
- [23] Z. Zhang and N. Troje, "3D Periodic Human Motion Reconstruction from 2D Motion Sequences," in *Computer Vision and Pattern Recognition Workshop, CVPRW '04*, pp. 186–186, June 2004.
- [24] M. Skolnik, *Introduction to Radar Systems*. McGraw-Hill, 2002.
- [25] J. Geisheimer, E. Greneker, and W. Marshall, "High-resolution Doppler model of the human gait," in *Proceedings of SPIE*, vol. 4744, 2002.
- [26] P. Stoica, *Introduction to spectral analysis*. Prentice Hall, 1997.
- [27] "GNU Radio." <http://gnuradio.org/redmine/wiki/gnuradio>. Last accessed on January 2011.
- [28] N. Manicka, "GNU radio testbed," Master's thesis, University of Delaware, 2007.
- [29] M. Ettus, *USRP users and developer's guide*. Ettus Research LLC.
- [30] "Universal Software Radio Peripheral." <http://www.ettus.com/>. Last accessed on January 2011.
- [31] L. K. Patton, "A GNU radio based software-defined radar," Master's thesis, Wright State University, 2007.
- [32] B. Godana, "Human Movement Characterization in Indoor Environment using GNU Radio Based Radar," Master's thesis, Delft University of Technology, 2009.